First fully ab initio potential energy surface of methane with a spectroscopic accuracy

A. V. Nikitin' , M. Rey, and Vl. G. Tyuterev

Citation: J. Chem. Phys. **145**, 114309 (2016); doi: 10.1063/1.4961973
View online: http://dx.doi.org/10.1063/1.4961973
View Table of Contents: http://aip.scitation.org/toc/jcp/145/11
Published by the American Institute of Physics

First fully *ab initio* potential energy surface of methane with a spectroscopic accuracy

A. V. Nikitin,[1,2,a)] M. Rey,[3] and Vl. G. Tyuterev[3]
[1]*Laboratory of Theoretical Spectroscopy, V.E. Zuev Institute of Atmospheric Optics, Russian Academy of Sciences, 1, Akademichesky Avenue, 634055 Tomsk, Russian Federation*
[2]*QUAMER Laboratory, Tomsk State University, 36 Lenin Avenue, 634050 Tomsk, Russian Federation*
[3]*Groupe de Spectrométrie Moléculaire et Atmosphérique, UMR CNRS 6089, Université de Reims, U.F.R. Sciences, B.P. 1039, 51687 Reims Cedex 2, France*

(Received 3 June 2016; accepted 19 August 2016; published online 21 September 2016)

Full 9-dimensional *ab initio* potential energy surfaces for the methane molecule are constructed using extended electronic structure coupled-cluster calculations with various series of basis sets following increasing X cardinal numbers: cc-pVXZ (X = 3, 4, 5, 6), aug-cc-ACVXZ (X = 3, 4, 5), and cc-pCVXZ-F12 (X = 3, 4). High-order dynamic electron correlations including triple and quadrupole excitations as well as relativistic and diagonal Born-Oppenheimer breakdown corrections were accounted for. Analytical potential functions are parametrized as non-polynomial expansions in internal coordinates in irreducible tensor representation. Vibrational energy levels are reported using global variational nuclear motion calculations with exact kinetic energy operator and a full account of the tetrahedral symmetry of CH_4. Our best *ab initio* surface including above-mentioned contributions provides the rms (obs.-calc.) errors of less than 0.11 cm^{-1} for vibrational band centers below 4700 cm^{-1}, and ~0.3 cm^{-1} for all 229 assigned experimentally determined vibrational levels up to the Icosad range <7900 cm^{-1} without empirically adjusted parameters. These results improve the accuracy of *ab initio* methane vibrational predictions by more than an order of magnitude with respect to previous works. This is an unprecedented accuracy of first-principles calculations of a five-atomic molecule for such a large data set. New *ab initio* potential results in significantly better band center predictions even in comparison with best available empirically corrected potential energy surfaces. The issues related to the basis set extrapolation and an additivity of various corrections at this level of accuracy are discussed. *Published by AIP Publishing.* [http://dx.doi.org/10.1063/1.4961973]

I. INTRODUCTION

Methane (CH_4), a high symmetry hydrocarbon, is one of the most important species for many domains of science and applications. Accurate knowledge of methane properties, quantum states, and transitions is crucial for the understanding of chemical bonds, molecular kinetics,[1–3] combustion process,[4] and environmental issues.[5,6] The intramolecular vibrational energy redistribution is a fundamental process for understanding the relations among vibrational motions and chemical reactions.[7]

In the Earth's atmosphere, methane contributes to climate changes acting as a greenhouse gas[8] and also affecting the ozone layer depletion.[9] In the solar system, the photochemistry of methane is responsible for the presence of numerous hydrocarbons in the giant planets.[10] It is a major absorber in the atmosphere of Titan (Saturn satellite).[11,12] Together with other elementary hydrocarbon molecules, methane dominates the opacity of some brown dwarfs and asymptotic-giant-branch (AGB) stars and plays a significant role in the physical chemistry of their outer atmospheres.[13,14,10] It is also considered among "standard" building blocks for carbon-rich atmospheres of many exoplanets.[15–17] Interpretation of spectral signatures of these recently observed objects requires accurate predictions of rovibrational bands, partition functions, and other thermodynamic properties[18] at high temperatures, which is a new challenge in astrophysics.[13,10,19] The detection of a methane emission at 3.3 μm in hot Jupiters was attributed to non-LTE (non-local thermodynamic equilibrium) mechanisms[20] involving transitions among very highly excited states. Obtaining a reliable potential energy surface (PES) of methane is a prerequisite to the study of related complex phenomena.

Analyses of highly excited vibration-rotation energy levels and transitions of the methane molecule are known to be a difficult task due to complex structures of vibrational polyads, numerous resonance perturbations, and high dimensionality of the calculation models.[21,23,120] Despite a significant progress in analyses of methane infrared spectra for $^{12}CH_4$[24,25,21,26,27] and for minor isotopologues[28–32] (the reference list being no exhaustive), the information on high-energy levels remains insufficient. Purely empirical extrapolations towards high-energy vibration states are not enough reliable facing problems of mathematically ill-defined parameters corresponding to the resonance coupling of various modes.[33,34] Though emission/absorption spectra measurements[35–38,19,39] at elevated temperatures and at higher wavenumber ranges[40–42] have been reported in the literature, the most of corresponding rovibrational patterns remain

---

[a)] Author to whom correspondence should be addressed. Electronic mail: avn@iao.ru. Tel.: +3822 - 491111-1208.

yet unassigned that prevents experimental determination of a sufficiently complete energy level set for astrophysical applications as was outlined in Refs. 19 and 38.

In the case of triatomics, very accurate *ab initio* calculations of potential energy surfaces (PESs) and of dipole moment surfaces (DMSs) led to a breakthrough in the extension of spectra analyses towards higher energy ranges. This was, for example, the case of water,[43–46] the carbon dioxide,[47,48] hydrogen sulfide,[50,51] and sulfur dioxide[52] spectroscopy as well as of the ozone spectra analyses.[22,53,54] In the latter case, *ab initio* predictions were mandatory for understanding the PES properties in the transition state range toward the dissociation threshold.[22,55,54] Many of *ab initio* PESs have been subsequently refined by a fit to experimental data to achieve better accuracy in line positions. Theoretical line lists for ammonia[56,49] and phosphine[57–59] are successful examples of such trend for four-atomics. New PESs and DMSs have been recently reported for five-atomic[60,61] and six-atomic molecules.[62–64]

A lot of effort has been devoted to electronic structure calculations of methane PES[65–73] and DMS.[74–76] Lee *et al.*,[69] have derived *ab initio* quartic force field with the cc-pVTZ basis sets. Marquardt and Quack[77,70] have constructed a model PES for large amplitude nuclear motions and reactions in methane based on earlier *ab initio* calculations of Lewerentz *et al.*[78,79] at about 660 points with a subsequent adjustment of parameter values. Schwenke and Partridge[71,80] have extended sophisticated calculations of methane PES with various basis sets and provided valuable insight to different *ab initio* methods and to related issues. They developed a full 9D approximation through eight-order analytical expansion, which was further used in many other works[81–84] as a benchmark surface for nuclear motion variational calculations. Oyanagi *et al.*[85] studied vibrational levels from the PES computed at the CCSD(T)/cc-pVTZ and MP2/cc-pVTZ level of theory. The present authors have computed potential and dipole moment surfaces of methane at about 20 000 nuclear configurations using CCSD(T) method with cc-pCVQZ basis set including relativistic contributions and also one-dimensional (1D) cc-pACV5Z radial corrections (Nikitin *et al.*[72]). Recently Majumder *et al.*[73] have reported new methane PES obtained from nearly 100 000 *ab initio* points calculated using multi-reference method with explicitly correlated basis set at the (AE)-MRCI-F12(Q)/CVQZ-F12 level. Their surface was created using multi-expansion interpolative fit and expansions in permutation invariant polynomials.

Despite these advanced studies in electronic structure theory, the best available *ab initio* methane PESs resulted in root-mean-squares (rms) errors of about 2–3 cm^{-1} for low-lying vibration levels in the range involving fundamental bands (below 3200 cm^{-1}), the error gradually increasing towards higher energies. This was much less accurate in comparison with triatomics and insufficient for new spectra assignments.

For this reason, many spectroscopic and dynamical studies employed empirically adjusted surfaces.[86,70,87,88,72] Yurchenko *et al.*[89] fitted their PES using experimental levels up to $J = 4$ whereas Wang and Carrington[88] have empirically optimized the *ab initio* PES of Schwenke[71] including experimental vibration levels up to about 6000 cm^{-1}. In our previous work, we have scaled four quadratic parameters of the analytical PES *ab initio* representation to four experimental fundamental frequencies. This empirically corrected surface will be referred to as NRT-2011 PES (Nikitin, Rey, and Tyuterev[72]) in what follows. Empirically adjusted PESs have been used for isotopic calculations[90–92,88] including CH_3D, CH_4, $^{13}CH_4$, CH_2D_2, and CHD_3 and for the generation of high-temperature predictions: ExoMol line list by Yurchenko and Tennyson[89] at 1500 K and Reims-Tomsk list up to 2000 K by Rey *et al.*[93,94] Prior these works, Warmbier *et al.* published 1000 K calculations within some approximated model.[95] Note however that these studies resulted in quite significant differences between theoretical rotationally resolved spectra simulations[89,93,94,38] and that large discrepancies were found in high-T vibration-rotation partition functions depending on the PESs and on calculation methods.[96,89,18,97]

In this study, we explore the state-of-art *ab initio* theory to better understand the role of various contributions and of basis sets and to approach the "spectroscopic accuracy" in high-energy vibrational levels. The latter term is traditionally used in theoretical works when the errors of calculations are significantly smaller than a typical distance between vibrational band centers that makes possible an unambiguous assignment of bands in observed spectra. The manuscript is structured as follows. The sampling (grids of points) of nuclear configuration space and electronic structure calculations accounting for various basis sets, for high-order electron correlations, for relativistic, and for diagonal Born-Oppenheimer breakdown corrections (DBOCs) are described in Section II. Section III is devoted to the surface parametrization using full T_d symmetry properties and to the analytical PES representation as a non-polynomial expansion in internal coordinates. Variational nuclear motion calculations with exact kinetic energy operator (EKO) and with various *ab initio* PESs constructed in Sec. III are considered in Section IV. Our best *ab initio* PES including above-mentioned contributions provided the rms (obs-calc) errors of less than 0.1 cm^{-1} for vibrational band centers below 3500 cm^{-1}, and ∼0.3 cm^{-1} for all 229 assigned experimentally determined vibrational levels up to the Icosad range ($\nu < 7900$ cm^{-1}). These results improve the accuracy of *ab initio* methane vibrational predictions by more than an order of magnitude with respect to previous works. The largest (obs.-calc.) error in the centers of five-quanta bands is now 1 cm^{-1}. Beyond four-atomic molecules, this is an unprecedented accuracy of first-principles calculations for such a large sample of data and is even much better than that of all available empirically optimized PESs of methane. Accuracy issues related to the basis set extrapolations that could be relevant to further extension of accurate *ab initio* calculations for other molecules are discussed in Section V.

II. ELECTRONIC STRUCTURE *AB INITIO* CALCULATION

The purpose of this work was to construct as accurate as possible fully *ab initio* PES of the methane molecule by using state-of-art electronic structure calculations. Our previous study[72] has shown that the coupled-cluster (CC) method[98] could provide quite a smooth shape of the methane PES that resulted in relatively small homogeneous error trends in vibrational energies. It was then possible to significantly reduce these errors by an empirical scaling of only four quadratic PES parameters. The present *ab initio* study aims at understanding the role of the basis set effects, of electronic correlations, and of various high-level corrections for this important molecule in order to quantify missing contributions and to obtain purely *ab initio* shape of the PES that provides sub-wavenumber accuracy for vibrational band centers without empirically adjusted parameters.

A. Basis sets and grids of nuclear configurations

As the first part of the study, we have computed *ab initio* electronic energies with the CCSD(T) method using hierarchical one-particle basis sets established by Dunning *et al.*[99] with increasing cardinal number X. The first series of calculations corresponded to frozen core cc-pVXZ basis set types that will be referred to as VXZ sets in abbreviated notations: VTZ, VQZ, V5Z, and V6Z. It was found that the account for augmented orbitals and for core-valence correlations results in a quite large effect on vibrational energies. All electrons were optimized in the corresponding series of calculations using aug-cc-ACVXZ core-valence basis sets with X = 3, 4, and 5 (denoted simply as ACVTZ, ACVQZ, and ACV5Z).

It has been recently claimed that the use of explicitly correlated methods[100,101] could improve the PES accuracy with fewer one-particle basis cardinal numbers. We thus computed electronic energies with the explicitly correlated F12 coupled cluster method CCSD(T)-F12B[101] in conjunction with the family of the F12-optimized correlation consistent polarized basis sets. In these calculations, the diagonal fixed amplitude ansatz 3C(FIX) (beta = 1.0)[102] was used. Next, our series were produced for two sets: with frozen core cc-pVTZ-F12 and cc-pVQZ-F12 and with all electron calculations using core-valence sets cc-pCVTZ-F12 and cc-pCVQZ-F12. In what follows these latter ones will be denoted as VTZ-F12, VQZ-F12, CVTZ-F12, and CVQZ-F12. The most of the calculations were carried out with MOLPRO programs package versions 2010.1 and 2012[103] unless stated otherwise.

It is well-known that the calculations with large basis sets are extremely demanding. Here we applied the same tensor techniques for an optimal sampling of the grid of nuclear configuration as described in the previous works.[104,72] This permitted accounting for the full tetrahedral (T_d) symmetry of the molecule to reduce the number of points. The extent of the grid points was chosen in a way that a maximum number of parameters of our analytical PES representation (Section III) would be well-defined in the least-squares fits to *ab initio* electronic energies. PES parameters responsible for the coupling of various vibrational modes were systematically included. The corresponding reference grid ($G^{(R)}$)[72] contained 19 982 points up to about 20 000 cm^{-1} above the equilibrium configuration. Very expensive calculations for the largest basis sets V6Z and ACV5Z were possible on a smaller grid ($G^{(S1)}$) of about 3100 geometries. Reduced grid samples were also applied for the evaluation of various corrections and for the extrapolation tests (see below).

B. Relativistic corrections

Contributions of the scalar relativistic effects were evaluated using various ansätze. As a first approach, we computed these corrections according to Douglas-Kroll-Hess[105] as the difference between DKROLL = 1 and DKROLL = 0 PESs with the VTZ basis. The corresponding one-dimensional (1D) sections were also computed with VQZ, VQZ-DK, and ACVQZ to control the basis set convergence for the relativistic contributions (see Fig. 1). As a supplementary test, we also computed electronic energies with the ACVQZ basis sets including MVD ("mass velocity" + Darwin) method.[106] The comparison in Fig. 1 shows a general consistency of all these calculations, three latter basis sets VQZ, VQZ-DK, ACVQZ giving very similar results. The MVD calculations with the VQZ basis sets were found indistinguishable from those obtained with Douglas-Kroll method.

C. Diagonal Born-Oppenheimer corrections (DBOCs)

Above-mentioned calculations were carried out within the Born-Oppenheimer (BO) approximations resulting in PESs independent on nuclear masses. It has been argued in many works[80,56] that the effects going beyond BO approximations need to be included in electronic structure calculations to approach the spectroscopic accuracy. The first-order diagonal Born-Oppenheimer corrections (DBOCs)[107] that bring mass-dependent contributions to the PES were computed here using the CCSD method as implemented in CFOUR program.[108] Because of its expense, the 9D calculations were done with the VTZ basis on a reduced grid of geometries (($G^{(S2)}$), 5000 points). The basis set convergence was checked for the 1D radial r(CH) section with the VQZ basis that gave practically the same DBOC results as for VTZ (see Fig. 1).

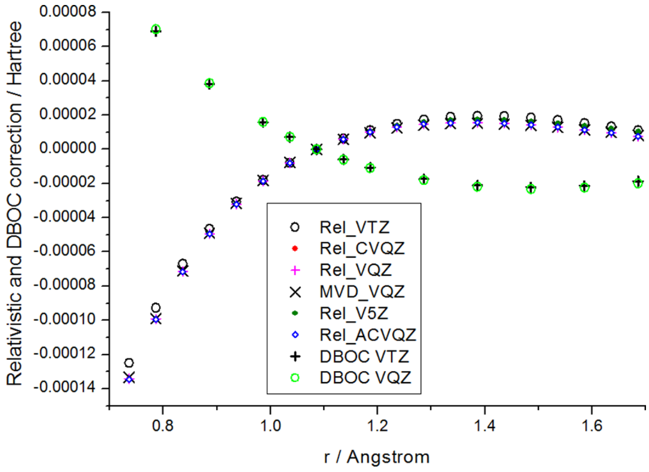

FIG. 1. Radial 1D PES cuts for scalar relativistic and diagonal Born-Oppenheimer corrections for various basis sets.

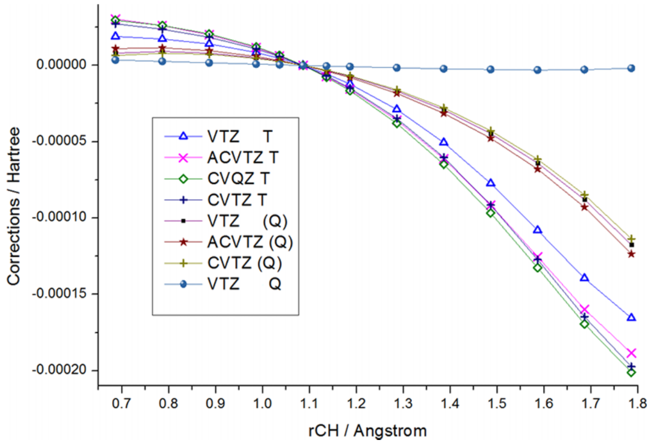

FIG. 2. Effect of higher-order (HO) electron correlations for the radial cut of the PES.

D. Higher-order (HO) dynamic electron correlations

In the CCSD(T) calculations using MOLPRO program, the dynamic electronic correlations corresponding to triple excitations were accounted for via the perturbation theory.[108] Recently it has become possible[109,108] to include quadrupole interactions in the coupled cluster method. The corresponding methods denoted as CCSDT, CCSDT(Q), and CCSDTQ have been implemented in the public version of MRCC[110] and in CFOUR programs.[108,109] Energy corrections due to high-order correlations computed in this work can be split in two parts $\Delta(\mathrm{HO}) = \Delta\mathrm{T} + \Delta(\mathrm{Q})$ were $\Delta\mathrm{T} = \mathrm{CCSDT} - \mathrm{CCSD(T)}$ and $\Delta(\mathrm{Q}) = \mathrm{CCSDT(Q)} - \mathrm{CCSDT}$. These calculations are quite expensive and were carried out here with the VTZ basis set for the reduced 9D geometry grid ($(\mathrm{G}^{(S2)})$, 5000 points). Only one-dimensional calculation of the ΔT correction was done with the CVTZ basis to check the basis set dependence (see Fig. 2).

In our previous work,[72] we have considered the scalar relativistic correction to the equilibrium geometry. An account for the DBOC and HO-correlations produces slight increase[111] of the equilibrium CH bond length giving the value $r_e = 1.086\,25$ Å in the present calculations (Fig. 3). This value is close to the estimations of Refs. 69 and 111.

III. ANALYTICAL REPRESENTATION FOR THE PES

For the full account of high tetrahedral symmetry of the methane molecule, the analytical representation of the nine-dimensional PES was constructed using T_d irreducible tensor formulation as described in our previous works.[72,112] Mass-dependent orthogonal coordinates with nuclear mass values were used involving stretching $\{r_i\}$ and angular $\{q_{ij}\}$ variables according to the definitions of Ref. 72. In order to construct the PES expansion, we defined suitable elementary analytical functions for each radial (stretching) and angular coordinate

$$\phi(r) = 1 - \exp[-1.9 * (r_i - r_e)], \tag{1}$$

$$\phi(q) = \cos(q) - \cos(q_e). \tag{2}$$

Symmetrized powers involving non-linear elementary functions (1,2) were built according to the coupling scheme of the irreducible tensor operators (ITOs) as described in Ref. 113. Reviews of the ITO techniques with applications to the tetrahedral molecules can be found in Refs. 114–117. The full 9D PES is represented by a linear combination of these tensors associated with PES parameters fitted to *ab initio* electronic energies.

A. Parameterization of the PES and of the PES-corrections

The maximum power of the symmetrized coordinates involved is called the order of the PES expansion. Note that a finite order analytical PES representation is a non-polynomial function with respect to the radial and angular coordinates and tends to the constant value for r → ∞ due to the asymptotic property of the morse-type function (1). The 6-order PES constructed in this way contains 287 expansion parameters. In order to fit our *ab initio* points at the full reference grid of 19 982 geometries, we added selected additional terms: 43 angular 7th order and 8th order parameters augmented with 10 parameters depending on the symmetrized combination of six angles $Q = \Sigma(\cos q_{ij})$ according to the formulation of Ref. 112.

Various small *ab initio* corrections described in Secs. II B and II C were computed on smaller reduced grids of geometries. We found that it was sufficient to fit their values with the second order (6 parameters) or with the fourth order (55 parameters) expansions.

B. Two versions for the geometry range expansions

As was already mentioned in Sec. II A, only restricted samples of geometries were included in our calculations for the largest ACV5Z and V6Z basis sets, which are very demanding in terms of CPU time and memory requirements. In order to expand these results to our full reference grid of 19 982 geometries, we have tested two approaches.

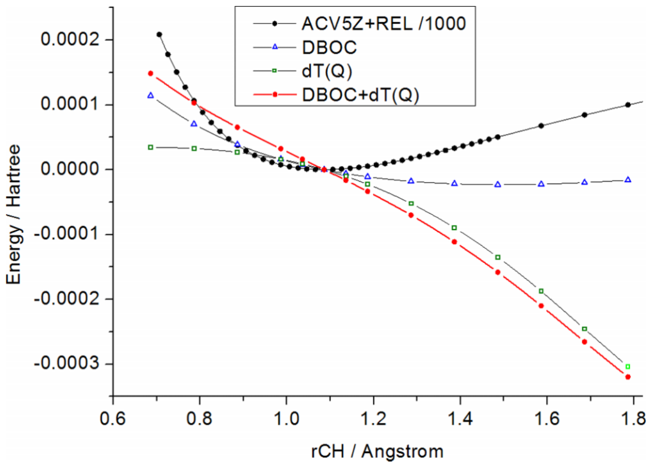

FIG. 3. Radial cuts for the methane CCSD(T) PES with scalar relativistic contributions (black dots) and for diagonal Born-Oppenheimer corrections (triangles). The contributions of higher order Δ(HO) triple and quadrupole electronic correlations are shown by empty squares. The sum of DBOC and HO corrections is given in red dots. Note that the BO PES radial section is divided by 1000 in order to fit the scale of the figure.

1. *First approach*

Let (S_i) symbolize the sets of symmetrized internal coordinates for which ACV5Z electronic energies were directly computed with MOLPRO. On the corresponding grid $G^{(S1)}$ of 3100 available *ab initio* points, we computed the energy differences diff$_2$(S_i) = ACV5Z-V5Z involving two basis sets. These differences, which can be viewed as the energy corrections due to the account of augmented orbitals and of core-valence correlation at X = 5 cardinal number, may be also denoted as diff$_2$ = $\Delta_{AC}(5)$. They were found to behave quite smoothly with respect to geometries and were possible to be modeled analytically using the second- or the forth-order expansions in symmetrized internal coordinates. We have checked that two latter fits gave very similar diff$_2$ values on our full reference grid $G^{(R)}$ of 19 982 points. As the full-grid calculations directly using MOLPRO with the V5Z basis set are now available (Sec. II A), this permits evaluating the electronic energies ACV5Z = diff$_2$ + V5Z for all remaining geometries.

2. *Second approach*

We have also applied the geometry expansion procedure involving four basis sets using the energy differences diff$_4$(S_i) = (ACV5Z-V5Z) – (ACVQZ-VQZ) on the smaller grid $G^{(S1)}$ of 3100 points for which the largest ACV5Z calculations were performed. This contribution, which can be written as diff$_4$ = $\Delta_{AC}(5) - \Delta_{AC}(4)$, represents a variation of the AC corrections with the augmentation of the cardinal number from X = 4 to X = 5 and is supposed to be quite small. Again for 3100 available ACV5Z points, the diff$_4$ was modelled as an analytical PES corrections. As the direct MOLPRO calculations on $G^{(R)}$ with the VQZ, V5Z, and ACVQZ are now available (Sec. II A), this also permits evaluating the electronic energies ACV5Z = diff$_4$ + (ACVQZ-VQZ) + V5Z for all remaining geometries.

C. Geometry expansion tests with lower cardinal numbers

The validity of both approaches can be checked on the entire grid $G^{(R)}$ if we go down by one cardinal number X ⇒ X – 1 in all basis sets involved in diff$_2$ and diff$_4$. In such test calculations, diff$_2$ = $\Delta_{AC}(4)$ = ACVQZ-VQZ and diff$_4$ = $\Delta_{AC}(4) - \Delta_{AC}(3)$ = (ACVQZ-VQZ) – (ACVTZ-VTZ). We then proceeded according to the same scheme exactly as in Sec. III B. These energy differences were first fitted analytically with the fourth order expansion on the smaller grid $G^{(S1)}$ of 3100 points and extended then to the full grid $G^{(R)}$. As all 19 982 points for the fours basis sets ACVQZ, VQZ, ACVTZ, VTZ were included in our direct *ab initio* MOLPRO calculations, we can compare the geometry expansion errors for these two methods on $G^{(R)}$.

The first *diff*$_2$-*approach* gave somewhat better results both for the analytical expansion and for the RMS quality of the fit. An illustration of this scheme is given in Fig. 4: the left-hand part of the diagram below the vertical line at 6000 cm^{-1} corresponds to the small $G^{(S1)}$ grid and the right-hand side corresponds to the errors of this method for analytic PES continuation. The RMS deviation (analytical PES–MOLPRO energies) for the ACVQZ test was 2.37 cm^{-1} for all 19 982 geometries. This is about four times larger than the RMS deviations of the fit including all these points where most of the fit errors were below 1 cm^{-1}.

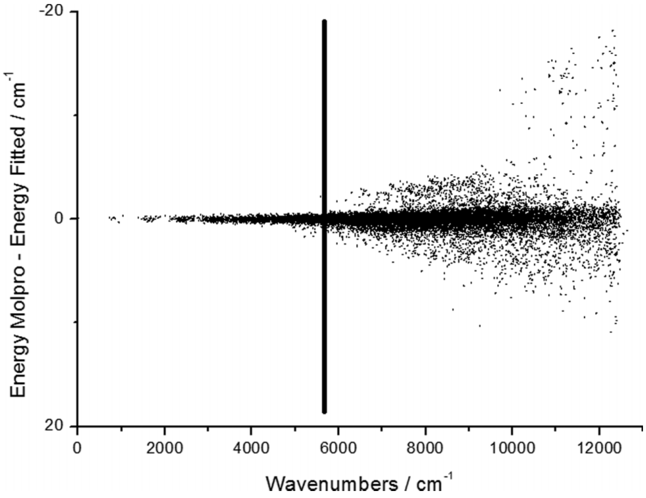

FIG. 4. Difference between electronic ACVQZ energies directly computed using MOLPRO and the PES obtained via the analytical prolongation of Δ_{AC} (4) + VQZ as discussed in test calculations of Sec. III C. The geometries of the left-hand part of the diagram below the vertical line at 5800 cm^{-1} correspond to the small $G^{(S1)}$ grid and the right-hand side corresponds to the errors on extended geometries (see Sec. III B). The RMS deviation (analytical PES–MOLPRO points) for the ACVQZ test was 0.16 cm^{-1} for the reduced grid below 5800 cm^{-1} and 2.37 cm^{-1} for all 19 982 geometries.

The second criterion for the choice of the method was based on the smoothness of the resulting ACV5Z surface, which was determined by the simultaneous weighted fit of 3100 "exact" *ab initio* energies and of 16 882 points obtained via $G^{(S1)} \Rightarrow G^{(R)}$ analytic expansion. The *diff*$_2$*–approach* also shows slightly less erratic behavior with better RMS fit deviation than the *diff*$_4$*–pproach*.

Finally, we have also examined the effect of the related approximations on the vibration levels computed with both PES versions (Sec. IV). The discrepancies between vibrational energies computed with *diff*$_2$ and *diff*$_4$ were found negligible up to the Octad range (range below 4700 cm^{-1}). Some noticeable distinctions appeared only at the Icosad range (above 6300 cm^{-1}) but the RMS (obs.-calc.) deviations were nearly the same.

IV. VARIATIONAL CALCULATIONS OF VIBRATION ENERGIES

The high tetrahedral symmetry of the CH_4 nuclear motion Hamiltonian results in two- and three-fold degeneracies in vibration-rotation levels and leads to sets (polyads) of nearby states of increasing dimension towards the range of overtone and combination bands. The polyad structure of the methane molecule is essentially governed by the quasi-coincidence of the stretching fundamental frequencies $\nu_1(A_1) \approx \nu_3(F_2) \approx 2\nu_2(E) \approx 2\nu_4(F_2)$[114,115] where notations A_1, E, and F_2 stand for irreducible representations of the T_d point group. This ratio is often referred to as 2:1:2:1 type resonance in harmonic vibrational modes. The polyads P_n are defined by an integer n expressed in terms of the principal vibrational quantum numbers as $n = 2(v_1 + v_3) + v_2 + v_4$. Methane vibrational polyads in successive wavenumber ranges are schematically shown in Figure 5: Ground State (GS = P_0, from microwave to 900 cm^{-1}), Dyad (P_1, 1100-1700 cm^{-1}), Pentad (P_2, 1800-3200 cm^{-1}), Octad (P_3, 3300-4700 cm^{-1}), Tetradecad (P_4, 4800-6200 cm^{-1}), Icosad (P_5, 6300-7900 cm^{-1}), and so on.

Due to anharmonic interactions among vibrational modes, the vibration levels of methane are split in sub-levels whose number (also given in Fig. 5) rapidly increases with energy. This is yet a simplified presentation as every vibration sub-level possesses rotational states that form complicated patterns strongly coupled by Coriolis and anharmonic resonances. These interactions can lead to bifurcations in ro-vibrational states at high V and J quantum numbers.[118–120] Corresponding perturbations in congested infrared spectra make their analyses extremely difficult. The reader can find detailed discussions in original papers[25,21,24] (and references therein) on the assignment and fitting of experimental spectra using spectroscopic polyad models. A recent overview of methane polyads and of related issues is given in Refs. 21 and 120.

In recent decades, methane has been used as a benchmark molecule for testing and validation of theoretical methods[121,122,82,88] for global vibrational and vibration-rotational calculations from multi-dimensional PESs. In addition to the works already referenced in the Introduction,[80,69,72,75,73] many other studies have contributed to this field of computational spectroscopy. Carter, Bowman *et al.*[123,82] have developed MULTIMODE program suite based on Watson Hamiltonian.[124] Wang and Carrigton[121,84] and Matyus *et al.*,[83] have studied convergence properties of variational calculations. The quantum dynamics algorithm with application to calculations of CH_4 vibrational levels was reported by Yu.[125,126] Most of the corresponding studies at that time employed *ab initio* PES constructed by Schwenke.[71] Variational methane calculations up to $J = 50$ using NRT-2011 empirically scaled PES[72] have been reported by Rey *et al.*,[23,93,127] with the Eckart frame Hamiltonian and the normal mode expansions.[117] Nikitin *et al.*[112] have shown that vibrational predictions of the latter approach are consistent with the rigorous variational method using exact KEO in internal coordinates (without PES truncation) at least up to the Icosad range. These both studies[23,112] were carried out in the tensor representations[128,129,117] for the nuclear motion Hamiltonian with a full account of the T_d symmetry.

Wang and Sibert[87,81] have shown that Contact Transformation (CT) method based on the perturbation theory and normal mode expansions provides an efficient alternative to variational approach. They have obtained an empirical

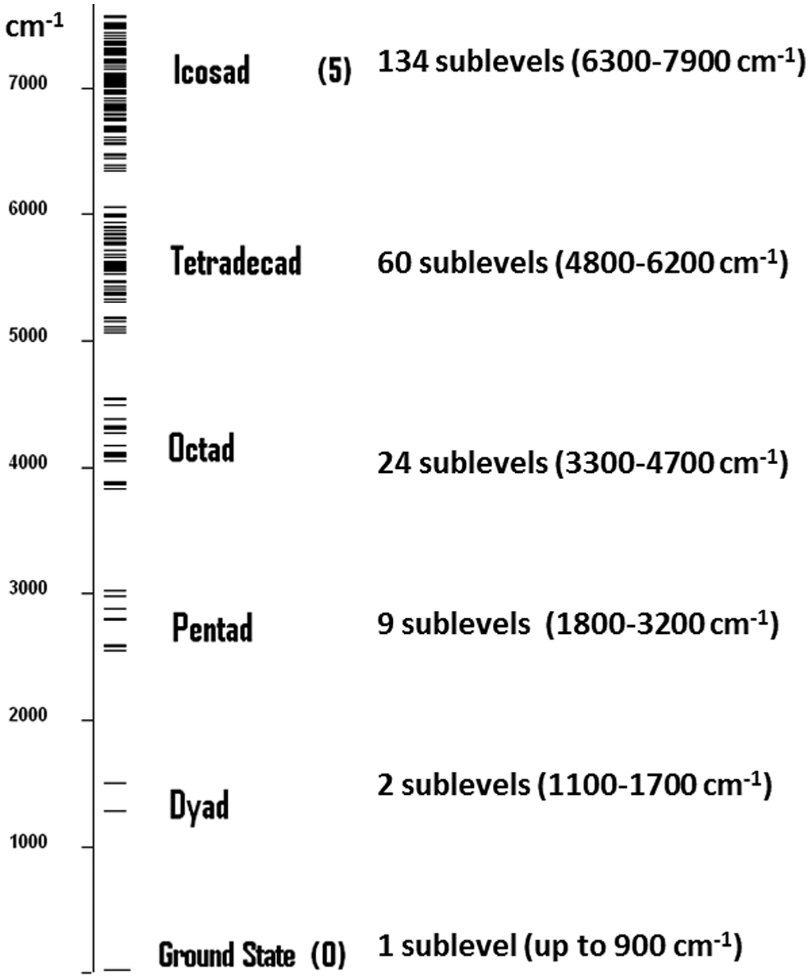

FIG. 5. Scheme of vibrational level patterns of the polyads with the vibration sublevels.

polynomial PES[81] by a simultaneously fit of anharmonicity parameters to the observed data of methane isotopologues. Tyuterev *et al.*[120] have derived vibrational levels up to twelve's methane polyad (P_{12}) corresponding to $E_{vib} \sim 18\,000$ cm^{-1} using high-order formulations of the CT method suggested in Ref. 130. The accuracy of this latter model was comparable to best variational calculations that made it possible to study[120] conical intersections of "rotational energy surfaces"[131,118] and qualitative changes[119] in high-J rovibrational patterns of methane polyads from the molecular potential function. Cassam-Chenai *et al.*[74,132] have considered another version of the quasi-degenerate perturbation theory for rovibrational methane levels also using NRT-2011 PES.[72]

For the calculations of the band centers, we employed here a variational method using exact nuclear KEO in orthogonal coordinates and "6A" symmetry-adapted contracted angular basis sets described in our previous work.[112] Vibrational basis sets denoted as X4 and X5 in Ref. 112 (with dimensions 25 000 and 31 000 correspondingly) provided the basis convergence errors of ~0.005 cm^{-1} up to the Octad (<4800 cm^{-1}) range that is comparable to the accuracy of "experimental" energy levels determination. Convergence precision is estimated as ~0.02 cm^{-1} in the Tetradecad region (4800-6300 cm^{-1}) and as ~0.05–0.2 cm^{-1} in the Icosad range up to 7900 cm^{-1}.

CCSD(T) calculations using various basis sets but without DBOC, relativistic, and high-order corrections will be referred to as "basic" *ab initio* results. Comparisons of vibrational levels computed at this level of the theory with observations are given in Table I. They show that the spectroscopic accuracy was not achieved even with augmented core-valence quintuple basis set (ACV5Z) and with explicitly correlated CVQZ-F12 when all electrons were optimized. The contributions of DBOC and relativistic corrections as well as of high-order dynamic electron correlations described in Secs. II A–II C are given on the left-hand side of Table II and in the upper panel of Figure 6. The contribution of HO electron correlation dT(Q) = CCSDT(Q) − CCSD(T) is clearly important being

TABLE I. Observed and calculated energy levels for the range of Dyad, Pentad (gray shaded), and Octad of $^{12}CH_4$ without corrections.

		Obs.–"basic" *ab initio*[b]							
Vib. state ($v_1v_2v_3v_4$) Γ	Obs. levels[a]	vtz	vqz	v5z	acvtz	acvqz	acv5z Comb2 o4	CVTZ-F12B	CVQZ-F12B
(0001)F2	1310.758	−1.01	−0.51	−0.01	−3.40	−0.81	−1.30	−2.02	−1.85
(0100)E	1533.330	0.02	0.66	0.86	−1.15	−0.29	−0.95	−1.27	−1.53
(0002)A1	2587.048	−2.78	−1.01	0.10	−4.59	−1.52	−2.66	−3.89	−3.69
(0002)F2	2614.261	−2.05	−0.94	0.06	−6.03	−1.59	−2.65	−4.02	−3.75
(0002)E	2624.617	−2.75	−1.15	0.00	−5.58	−1.54	−2.60	−3.98	−3.67
(0101)F2	2830.315	−1.36	0.03	0.82	−2.89	−0.95	−2.30	−3.24	−3.38
(0101)F1	2846.074	−0.98	0.18	0.84	−4.15	−1.12	−2.30	−3.30	−3.42
(1000)A1	2916.481	2.40	1.79	2.27	4.76	−0.14	−2.64	−2.71	−3.99
(0010)F2	3019.492	5.61	3.33	3.18	6.82	0.21	−2.45	−2.39	−4.04
(0200)A1	3063.647	−0.08	1.15	1.61	−1.36	−0.52	−2.00	−2.59	−3.14
(0200)E	3065.140	−0.04	1.25	1.65	−1.89	−0.55	−1.95	−2.56	−3.08
(0003)F2	3870.486	−4.33	−1.49	0.18	−5.90	−2.30	−4.13	−5.87	−5.62
(0003)A1	3909.186	−3.10	−1.29	0.19	−7.98	−2.35	−4.07	−6.02	−5.70
(0003)F1	3920.517	−3.75	−1.49	0.13	−7.41	−2.32	−4.01	−5.99	−5.64
(0003)F2	3930.921	−4.50	−1.72	0.06	−7.18	−2.28	−3.98	−5.96	−5.56
(0102)E	4101.392	−3.22	−0.58	0.84	−3.64	−1.67	−3.74	−5.17	−5.26
(0102)F1	4128.757	−2.65	−0.50	0.81	−4.82	−1.71	−3.74	−5.28	−5.34
(0102)A1	4132.869	−3.28	−0.73	0.73	−4.14	−1.68	−3.69	−5.26	−5.26
(0102)F2	4142.861	−2.21	−0.31	0.87	−5.75	−1.86	−3.73	−5.30	−5.36
(0102)E	4151.202	−2.79	−0.47	0.83	−5.45	−1.84	−3.68	−5.26	−5.30
(0102)A2	4161.838	−2.75	−0.46	0.82	−6.07	−1.89	−3.68	−5.30	−5.31
(1001)F2	4223.461	1.07	1.12	2.13	1.42	−1.04	−4.03	−4.83	−5.93
(0011)F2	4319.209	4.45	2.75	3.09	3.49	−0.67	−3.82	−4.50	−5.97
(0011)E	4322.189	4.18	2.59	3.01	3.45	−0.69	−3.80	−4.51	−5.94
(0011)F1	4322.588	4.28	2.62	3.01	3.51	−0.67	−3.81	−4.52	−5.96
(0011)A1	4322.694	3.88	2.47	2.91	3.17	−0.77	−3.89	−4.64	−6.04
(0201)F2	4348.717	−1.71	0.45	1.54	−2.20	−1.15	−3.41	−4.57	−5.02
(0201)F1	4363.609	−1.43	0.62	1.58	−3.26	−1.26	−3.38	−4.57	−5.01
(0201)F2	4378.950	−1.15	0.69	1.56	−4.33	−1.43	−3.42	−4.66	−5.08
(1100)E	4435.120	2.25	2.33	3.01	3.54	−0.50	−3.66	−4.03	−5.55
(0110)F1	4537.550	5.54	3.88	3.94	5.64	−0.16	−3.51	−3.77	−5.66
(0110)F2	4543.762	5.28	3.72	3.84	5.53	−0.21	−3.54	−3.84	−5.69
(0300)E	4592.037	−0.44	1.47	2.21	−1.44	−0.86	−3.17	−4.03	−4.86
(0300)A2	4595.270	−0.23	1.71	2.33	−2.25	−0.84	−3.03	−3.91	−4.70
(0300)A1	4595.504	−0.31	1.66	2.29	−2.38	−0.91	−3.08	−3.96	−4.75

[a] All values are given in wavenumber units (cm^{-1}). Experimental vibration levels are taken from Refs. 25 and 26.

[b] "Basic *ab initio*" calculations do not include DBOC, relativistic corrections, and high-order electronic correlations.

TABLE II. Vibration levels with contributions of relativistic, DBOC corrections, and high-order electron correlations for the Dyad, Pentad (gray shaded), and Octad ranges.

	This work										
		Contributions of corrections			Theoretical levels with corrections				MRCI, Ref. 73	
Vib. state ($v_1v_2v_3v_4$) Γ	Obs. levels[a]	Rel[b]	DBOC[b]	dT(Q)[b]	CVQZ-F12 + corr	Obs-calc	ACV5Z + corr	Obs-calc	Calc	Obs-calc
(0001)F2	1310.758	0.196	−0.465	−1.11	1311.28	−0.52	1310.715	0.042	1313.07	−2.31
(0100)E	1533.330	0.342	−0.181	−1.18	1533.87	−0.54	1533.297	0.032	1534.51	−1.18
(0002)A1	2587.048	0.375	−0.910	−2.20	2588.05	−1.00	2587.012	0.035	2591.54	−4.50
(0002)F2	2614.261	0.392	−0.918	−2.25	2615.29	−1.03	2614.175	0.085	2618.82	−4.55
(0002)E	2624.617	0.404	−0.923	−2.21	2625.64	−1.03	2624.551	0.065	2629.21	−4.60
(0101)F2	2830.315	0.521	−0.629	−2.28	2831.38	−1.06	2830.284	0.030	2833.70	−3.39
(0101)F1	2846.074	0.541	−0.646	−2.31	2847.15	−1.08	2846.018	0.055	2849.58	−3.51
(1000)A1	2916.481	0.059	−0.483	−2.20	2917.99	−1.51	2916.625	−0.144	2917.88	−1.40
(0010)F2	3019.492	−0.07	−0.159	−2.53	3020.87	−1.38	3019.273	0.218	3019.39	0.10
(0200)A1	3063.647	0.674	−0.349	−2.40	3064.78	−1.13	3063.632	0.014	3065.97	−2.33
(0200)E	3065.140	0.688	−0.361	−2.37	3066.24	−1.10	3065.103	0.036	3067.50	−2.36
(0003)F2	3870.486	0.571	−1.367	−3.34	3872.04	−1.55	3870.506	−0.020	3877.17	−6.69
(0003)A1	3909.186	0.595	−1.366	−3.42	3910.76	−1.57	3909.092	0.094	3915.93	−6.73
(0003)F1	3920.517	0.611	−1.378	−3.38	3922.09	−1.57	3920.418	0.098	3927.29	−6.78
(0003)F2	3930.921	0.622	−1.384	−3.34	3932.48	−1.56	3930.853	0.067	3937.75	−6.83
(0102)E	4101.392	0.703	−1.082	−3.38	4102.98	−1.59	4101.426	−0.034	4106.93	−5.54
(0102)F1	4128.757	0.730	−1.095	−3.43	4130.38	−1.63	4128.744	0.012	4134.38	−5.62
(0102)A1	4132.869	0.724	−1.100	−3.38	4134.48	−1.61	4132.874	−0.005	4138.51	−5.65
(0102)F2	4142.861	0.742	−1.106	−3.45	4144.49	−1.63	4142.810	0.050	4148.56	−5.70
(0102)E	4151.202	0.752	−1.114	−3.41	4152.82	−1.62	4151.164	0.037	4156.95	−5.75
(0102)A2	4161.838	0.772	−1.126	−3.43	4163.47	−1.63	4161.793	0.045	4167.65	−5.81
(1001)F2	4223.461	0.269	−0.951	−3.38	4225.50	−2.04	4223.566	−0.105	4227.24	−3.78
(0011)F2	4319.209	0.130	−0.632	−3.68	4321.14	−1.93	4318.958	0.250	4321.40	−2.19
(0011)E	4322.189	0.149	−0.628	−3.69	4324.11	−1.92	4321.946	0.242	4324.46	−2.29
(0011)F1	4322.588	0.147	−0.628	−3.70	4324.53	−1.94	4322.351	0.236	4324.88	−2.29
(0011)A1	4322.694	0.140	−0.654	−3.75	4324.61	−1.91	4322.429	0.264	4325.07	−2.37
(0201)F2	4348.717	0.850	−0.812	−3.48	4350.40	−1.68	4348.742	−0.025	4353.20	−4.49
(0201)F1	4363.609	0.891	−0.834	−3.49	4365.29	−1.68	4363.608	0.000	4368.16	−4.56
(0201)F2	4378.950	0.907	−0.851	−3.53	4380.66	−1.71	4378.943	0.006	4383.62	−4.68
(1100)E	4435.120	0.416	−0.678	−3.39	4437.20	−2.08	4435.277	−0.157	4437.79	−2.67
(0110)F1	4537.550	0.286	−0.347	−3.75	4539.53	−1.98	4537.353	0.197	4538.68	−1.14
(0110)F2	4543.762	0.296	−0.354	−3.78	4545.75	−1.99	4543.574	0.187	4544.95	−1.20
(0300)E	4592.037	1.044	−0.560	−3.62	4593.87	−1.83	4592.117	−0.080	4595.58	−3.56
(0300)A2	4595.270	1.064	−0.570	−3.57	4597.00	−1.73	4595.276	−0.006	4598.70	−3.44
(0300)A1	4595.504	1.071	−0.579	−3.57	4597.28	−1.78	4595.544	−0.040	4599.23	−3.73
RMS-deviation						1.55		0.11		4.17

[a] All values are given in wavenumber units (cm^{-1}).

[b] Contributions of *ab initio* corrections to vibration levels were found as the differences E_{vib} (ACV5Z + PES Corrections) - E_{vib} (ACV5Z PES); high-order correlation is computed as dT(Q) = CCSDT(Q) – CCSD(T).

larger than 3 cm^{-1}. The middle part of Table II gives the comparison between *ab initio* vibration levels accounting for these corrections and experimental levels up to the Octad range. The best results correspond to ACV5Z calculations involving DBOC, Douglas-Kroll, and dT(Q) effects. This will be denoted as (ACV5Z+) calculations in what follows.

Most recent *ab initio* results for CH_4 vibration levels computed by Majumder *et al.*[73] from MRCI methane PES up to the Octad range are given in the last two columns of Table II. Tables III and IV give comparisons of variational calculations using our (ACV5Z+) PES with bands centers deduced from analyses of experimental spectra[25,21,133–135] for higher energy ranges involving Tetradecad and Icosad. To our knowledge, no first principle predictions of vibration levels in these ranges have been published before this work. Table V presents the RMS (obs.-calc.) statistics for $^{12}CH_4$ vibration levels computed from our (ACV5Z+) and (CVQZ-F12B+) PESs in comparison with *ab initio* MRCI results[73] and with calculations from empirically corrected PESs.[72,88] It is clearly seen that the (ACV5Z+) PES does much better in this vibrational test and permits improving the accuracy of best available *ab initio* calculations by a factor of 35 in average.

Statistics for the most accurate available vibrational calculations from empirically corrected methane PESs reported in our previous work (NRT-2011[72]) and by Wang and Carrington[88] are given in last two columns of Table V. Detailed comparison tables are provided in supplementary material to the paper. It is instructive to note that the (ACV5Z+) PES

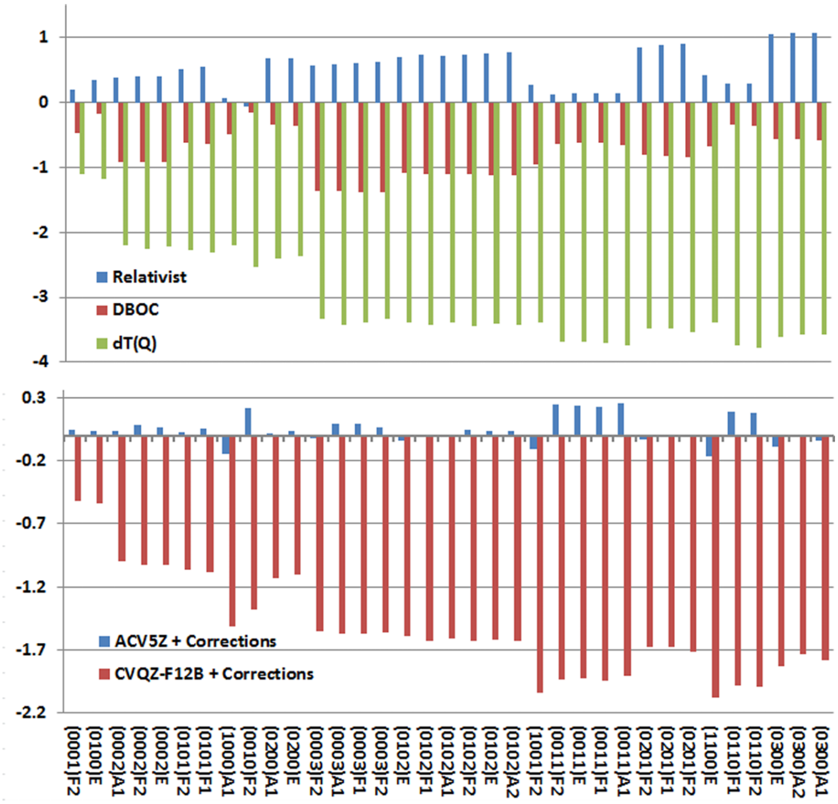

FIG. 6. Upper panel (a): contribution of relativistic effects, DBOC, and high-order electron correlations dT(Q) to vibrational energies up to octad. Lower panel (b): Obs.-Calc. errors in vibration levels for ACV5Z+ and CVQZ-F12B+ *ab initio* PESs including all contributions of the upper panel. Both vertical scales are given in cm^{-1}.

results in significantly better band centers calculations even in those ranges (Pentad to Tetradecad), which had been included in the empirical fit in Ref. 88. This suggests that high-level electronic structure methods are capable of producing more physically meaningful shapes of multi-dimensional PESs than empirical models. Note that the increasing (obs.-calc.) residuals in the Icosad range (from 0.167 cm^{-1} up to 0.375 cm^{-1}) could be partly due to larger uncertainties of band centers determination from experimental spectra: for some bands containing a small number of assigned transitions, these empirical uncertainties mounted to 0.1-0.4 cm^{-1} in worst cases.

Previous empirically corrected PES[72] combined with accurate *ab initio* DMS[76] and with related first principles intensity predictions[127] has recently permitted assigning 108

TABLE III. Empirical and *ab initio* vibrational energy levels of $^{12}CH_4$ for our best *ab initio* PES in the Tetradecad range. All values are given in wavenumber units (cm^{-1}).

Vib. state ($v_1v_2v_3v_4$) Γ	Expt. spectra analyses[a]	TW[b] *ab initio*	"Expt."-*ab initio* (TW)
(0004)A1	5121.718	5121.95	−0.24
(0004)F2	5143.365	5143.53	−0.16
(0004)E	5167.202	5167.36	−0.15
(0004)F2	5210.734	5210.69	0.03
(0004)E	5228.757	5228.73	0.01
(0004)F1	5230.598	5230.57	0.02
(0004)A1	5240.401	5240.41	−0.01
(0103)F2	5370.527	5370.72	−0.20
(0103)F1	5389.660	5389.81	−0.15
(0103)E	5424.779	5424.82	−0.04
(0103)F2	5429.867	5429.94	−0.08
(0103)F1	5437.312	5437.36	−0.05
(0103)F2	5444.667	5444.67	−0.01
(0103)F1	5462.795	5462.81	−0.02
(1002)A1	5492.679	5492.84	−0.17
(1002)F2	5521.409	5521.55	−0.14
(1002)E	5533.464	5533.46	−0.00
(0012)F2	5587.977	5587.75	0.22
(0012)A1	5604.936	5604.90	0.03
(0202)A1	5613.217	5613.21	−0.00

TABLE III. (*Continued.*)

Vib. state ($v_1v_2v_3v_4$) Γ	Expt. spectra analyses[a]	TW[b] *ab initio*	"Expt."-*ab initio* (TW)
(0202)E	5613.565	5613.58	−0.02
(0012)F2	5615.234	5614.98	0.25
(0012)F1	5615.747	5615.47	0.27
(0012)E	5619.273	5619.11	0.15
(0012)F1	5626.138	5625.93	0.20
(0012)F2	5627.289	5627.04	0.24
(0202)F2	5642.404	5642.53	−0.13
(0202)E	5654.273	5654.35	−0.08
(0202)F1	5655.853	5655.94	−0.09
(0202)A2	5663.973	5664.01	−0.04
(0202)F2	5668.669	5668.75	−0.08
(0202)A1	5681.598	5681.67	−0.07
(0202)E	5691.016	5691.10	−0.08
(1101)F2	5726.815	5726.96	−0.15
(1101)F1	5744.832	5745.01	−0.18
(2000)A1	5790.424	5790.34	0.08
(0111)F2	5823.126	5822.87	0.24
(0111)F1	5825.399	5825.23	0.16
(0111)E	5832.099	5831.93	0.16
(0111)A1	5834.785	5834.66	0.11
(0111)E	5842.636	5842.45	0.17
(0111)A2	5842.950	5842.77	0.17
(0111)F2	5844.100	5843.93	0.16
(0111)F1	5847.229	5847.04	0.18
(1010)F2	5861.303	5861.26	0.03
(0301)F2	5867.673	5867.76	−0.09
(0301)F1	5879.713	5879.86	−0.15
(0301)F2	5894.366	5894.54	−0.18
(0301)F1	5909.106	5909.30	−0.19
(1200)A1	5939.55	5939.71	−0.16
(1200)E	5952.444	5952.64	−0.20
(0020)A1	5968.00	5967.93	0.07
(0020)F2	6004.626	6004.30	0.31
(0020)E	6043.848	6043.47	0.37
(0210)F2	6054.605	6054.49	0.10
(0210)F1	6060.600	6060.49	0.10
(0210)F2	6065.583	6065.50	0.07
(0400)A1	6116.75	6117.12	−0.37
(0400)E	6118.53	6118.86	−0.33
(0400)E	6124.07	6124.28	−0.21
RMS-deviation			0.167

[a] "Expt.": band centers empirically determined from experimental spectra analyses.[21,133,97]

[b] TW: calculated from our *ab initio* (ACV5Z+) PES including relativistic, DBOC corrections, and high-order electron correlations.

new methane bands.[24] Also, the inter-modes resonance coupling parameters computed from the PES via the CT method[120] helped to avoid ambiguity issues[33,34] in the effective spectroscopic models and to advance in detailed spectra analyses.[27,32,133] We plan to use the new *ab initio* PES to extend this work for higher wavenumber and higher temperature ranges where the assignments are yet lacking for the most of experimentally recorded methane bands.[35–42]

V. DISCUSSION: ACCURACY ISSUES

During this study, various tests were carried out in order to understand the sources of remaining errors in methane *ab initio* calculations.

A. Accuracy of high-order dynamic correlations of DBOC and relativistic corrections

Scalar relativistic corrections were tested with higher basis sets (VQZ, VQZ-DK, and ACV5Z) at some representative samples of geometries. No significant changes were obtained in fundamental vibrational frequencies, suggesting that the errors in relativistic corrections were below 0.1 cm^{-1}, at least for the fundamental bands. The accuracy of high-order (HO) dynamic electron correlations due to the account of triple and quadrupole excitations in the coupled cluster method ($\Delta T = \text{CCSDT} - \text{CCSD(T)}$ and $\Delta(Q) = \text{CCSDT(Q)} - \text{CCSDT}$) was tested with ACVTZ and CVQZ basis sets for several 1D PES cuts. No significant changes were found with respect to HO computed in the CVTZ basis.

TABLE IV. Empirical and *ab initio* vibrational energy levels $^{12}CH_4$ bands centers for our best *ab initio* PES in the Icosad range.

Vib. state ($v_1v_2v_3v_4$) Γ	Emp.[a]	TW[b] *ab initio*	Emp.-calc
(0005)F2	6377.521	6378.21	−0.69
(0005)A1	6405.968	6406.59	−0.62
(0005)F1	6429.234	6429.80	−0.56
(0005)F2	6450.059	6450.58	−0.52
(0005)E	6507.406	6507.66	−0.26
(0005)F2	6507.554	6507.80	−0.25
(0005)F1	6529.770	6530.04	−0.27
(0005)F2	6539.182	6539.41	−0.23
(0104)E	6617.524	6618.11	−0.59
(0104)F1	6638.525	6639.12	−0.59
(0104)A1	6655.888	6656.42	−0.53
(0104)F2	6657.092	6657.62	−0.53
(0104)E	6680.934	6681.36	−0.43
(0104)A2	6682.781	6683.29	−0.51
(0104)F2	6717.991	6718.33	−0.33
(0104)F1	6721.985	6722.26	−0.28
(0104)E	6729.604	6729.97	−0.37
(0104)F2	6733.105	6733.44	−0.33
(0104)A1	6737.774	6738.01	−0.24
(0104)A2	6746.224	6746.52	−0.29
(0104)F1	6755.374	6755.65	−0.28
(0104)E	6766.230	6766.48	−0.25
(1003)F2	6769.194	6769.49	−0.30
(1003)A1	6809.456	6809.58	−0.12
(1003)F1	6822.291	6822.43	−0.14
(1003)F2	6833.190	6833.36	−0.17
(0013)F2	6858.707	6858.68	0.02
(0013)E	6862.74	6862.61	0.12
(0013)F1	6862.85	6862.72	0.12
(0013)A1	6863.10	6863.11	−0.01
(0203)F2	6869.793	6870.28	−0.48
(0203)F1	6889.68	6890.22	−0.54
(0013)F2	6897.383	6897.25	0.12
(0203)F2	6905.60	6906.13	−0.53
(0013)E	6908.80	6908.51	0.28
(0013)F2	6910.383	6910.16	0.22
(0013)F1	6915.18	6914.79	0.38
(0013)A2	6918.55	6918.37	0.17
(0013)F1	6921.58	6921.41	0.16
(0013)A1	6922.07	6921.95	0.11
(0013)F2	6924.967	6924.78	0.18
(0013)E	6925.67	6925.49	0.17
(0203)E	6938.40	6938.74	−0.34
(0203)A1	6940.051	6940.36	−0.31
(0203)F2	6940.10	6940.49	−0.39
(0203)F1	6945.16	6945.59	−0.43
(0203)F1	6949.70	6950.15	−0.45
(0203)F2	6962.42	6962.76	−0.34
(0203)F1	6972.86	6972.90	−0.04
(1102)E	6990.01	6990.29	−0.28
(0203)F2	6992.582	6992.96	−0.38
(1102)F1	7020.43	7020.71	−0.28
(1102)A1	7024.03	7024.23	−0.20
(1102)F2	7035.180	7035.39	−0.21
(1102)E	7045.69	7045.88	−0.19
(1102)A2	7056.56	7056.78	−0.22
(0112)F1	7085.637	7085.05	0.57
(2001)F2	7085.73	7085.59	0.13
(0112)F2	7097.915	7097.94	−0.02
(0112)E	7107.28	7107.22	0.05
(0112)A2	7114.54	7114.67	−0.13
(0112)F2	7116.385	7116.21	0.16
(0112)F1	7118.05	7117.59	0.45
(0302)E	7118.40	7118.91	−0.51
(0302)A1	7120.74	7120.94	−0.20
(0112)F2	7121.90	7121.41	0.48
(0112)F1	7130.90	7130.83	0.06
(0112)F2	7131.135	7131.04	0.09
(0112)A1	7132.50	7132.74	−0.24
(0112)E	7133.69	7133.89	−0.20
(0302)A2	7134.00	7134.17	−0.17
(0112)F1	7139.23	7139.14	0.08
(0112)F2	7141.50	7141.48	0.01
(0112)F1	7151.02	7150.80	0.21
(0302)F1	7153.84	7154.44	−0.60
(1011)A1	7157.16	7156.95	0.20
(1011)F2	7158.128	7158.07	0.05
(1011)E	7164.60	7164.82	−0.22
(1011)F1	7165.60	7166.40	−0.80
(0302)E	7168.00	7168.57	−0.57
(0302)F2	7168.422	7168.94	−0.52
(0302)A1	7176.10	7176.88	−0.78
(0302)F1	7180.00	7180.58	−0.58
(0302)F2	7191.05	7191.81	−0.76
(0302)E	7191.85	7192.39	−0.54
(0302)E	7217.40	7218.02	−0.62
(0302)A2	7221.10	7221.75	−0.65
(1201)F2	7225.433	7225.69	−0.25
(1201)F1	7246.01	7246.29	−0.28
(0021)F2	7250.542	7250.49	0.04
(1201)F2	7269.442	7269.58	−0.14
(2100)E	7295.20	7295.10	0.09
(0021)F1	7295.50	7295.55	−0.05
(0021)E	7295.80	7296.41	−0.61
(0021)A1	7299.443	7299.14	0.29
(0021)F2	7299.45	7299.17	0.27
(0211)F1	7326.25	7326.17	0.07
(0211)F2	7331.053	7330.95	0.10
(0021)F2	7337.55	7337.22	0.32
(0021)F1	7338.16	7337.87	0.28
(0211)A1	7341.60	7341.74	−0.14
(0211)E	7342.10	7342.08	0.01
(0211)F2	7346.006	7345.96	0.03
(0211)F1	7346.46	7346.48	−0.02
(0211)A2	7348.85	7348.88	−0.03
(0211)E	7352.20	7352.19	0.00
(0211)A1	7360.80	7360.84	−0.04
(0211)E	7362.16	7361.81	0.34
(0211)F2	7365.401	7365.41	−0.01
(0211)F1	7368.88	7368.86	0.01
(1110)F1	7373.16	7373.32	−0.16
(1110)F2	7374.246	7374.50	−0.25
(0401)F2	7384.108	7384.60	−0.49
(0401)F1	7394.20	7394.96	−0.76
(0401)F2	7408.20	7409.06	−0.86
(0401)F1	7422.30	7423.25	−0.95
(0401)F2	7436.30	7437.39	−1.09
(1300)E	7447.52	7448.00	−0.48
(1300)A2	7468.21	7468.60	−0.39
(1300)A1	7468.50	7468.88	−0.38

TABLE IV. (*Continued.*)

Vib. state ($v_1v_2v_3v_4$) Γ	Emp.[a]	TW[b] *ab initio*	Emp.-calc
(1300)E	7483.67	7483.71	−0.04
(0120)F2	7510.338	7510.16	0.17
(0120)F1	7512.26	7512.12	0.13
(0120)A2	7546.49	7546.11	0.37
(0120)E	7552.23	7551.97	0.25
(0120)A1	7559.00	7558.75	0.24
(0310)F1	7569.51	7569.68	−0.17
(0310)F2	7575.858	7576.02	−0.16
(0310)F1	7580.90	7581.05	−0.15
(0310)F2	7584.513	7584.69	−0.18
(0500)E	7640.81	7640.63	0.17
(0500)A2	7643.78	7644.03	−0.25
(0500)A1	7644.89	7644.90	−0.01
(0500)E	7651.68	7652.20	−0.52
RMS-deviation			0.37

[a] All values in cm^{-1}. "Emp": empirically determined J = 0 values from spectra analyses.[27,24].

[b] TW: calculated from our *ab initio* (ACV5Z+) PES including relativistic, DBOC corrections, and high-order electronic correlations.

The comparison of radial HO corrections for ACVTZ, CVQZ, CVTZ, VTZ(fc) permits to conclude that even an extrapolation of HO to ACVQZ basis would not change stretching vibration frequencies by more than 0.2 cm^{-1}. These corrections affect both ν_1 and ν_3 in a similar way. We do not claim that somewhat larger (obs.-calc.) deviations in vibration levels (Table II) obtained with CVQZ-F12 would prove a deficiency of the F12 approach because high-order correlations were not yet implemented with this basis set.

The changes between DBOC corrections using X = 3 and X = 4 basis sets were found negligible. Note that radial dependences of DBOC and relativistic contributions have opposite signs (Fig. 1), but they do not cancel completely. If both of them are neglected the errors in vibrational levels increase significantly.

B. Atomic basis set effects. Basis set extrapolation errors

It is less straightforward to evaluate the errors that can be caused by the basis set truncations and by a deficiency of CBS extrapolation schemes. According to well-known recommendations of the theory, the Hartree-Fock (HF) and correlation energies are to be extrapolated with different formulas when increasing the cardinal numbers X of one-electron basis sets. For the non-correlated reference energy of the VXZ sequences, it was found that the best match was given by the exponential law $E_{n.c.}^{(X)} = \alpha\, exp\,(-\beta X) + \gamma$. For the electron correlation energies, the best extrapolation with the atomic basis set cardinal number X was found to be given by the following inverse cubic law:[136–139]

$$E_c^{(X)} = a + b(X + p)^{-3}, \tag{3}$$

where the optimal value of the p parameter in Eq. (3) for our set of *ab initio* points was estimated to be $p = -0.6$. Indeed, the methane correlation energies $E_c^{(X)}$ plotted versus $(X - 0.6)^{-3}$ match quite precisely straight lines both for VXZ ($X = 3, 4, 5, 6$) and for ACVXZ ($X = 3, 4, 5$) basis sequences as shown in Fig. 7.

In order to evaluate the accuracy of the extrapolation formula (3), we have derived two parameters a and b of this linear regression from VTZ, VQZ, V5Z calculations using weighted fit. According to the estimated accuracy, the weights of VTZ, VQZ, V5Z data were chosen as ¼, ½, 1 correspondingly. With this test fit, the correlation energy was extrapolated to V6Z basis. For the equilibrium geometry, this extrapolation gave $E_c^{(X)}$ value of –0.001 144 a.u.(–251 cm^{-1}) whereas the direct *ab initio* V6Z calculation using MOLPRO produced a nearby result of –0.001 171 a.u. (–257 cm^{-1}).

The nuclear geometry dependence of the (V6Z-V5Z) difference in the correlation energy was found quite small with the variation amplitude of a few wave numbers. The comparison of the extrapolated (V6Z-V5Z) differences for $E_c^{(X)}$ using Eq. (3) with the "exact" (V6Z-V5Z) values directly computed by MOLPRO for various geometries is shown in Fig. 8 versus electronic energies. It is instructive to give this

TABLE V. Obs.-calc. RMS statistics for $^{12}CH_4$ vibration levels computed from recent methane PESs.

			Purely *ab initio* PESs			Empirically optimized PESs	
Polyad	Range (cm^{-})	N expt. vib. levels	Best TW[a] ACV5Z+	TW[a] CVQZ-F12B+	Majumder[b] Ref. 73, MRCI	NRT[72 c] Refs. 127 and 24	WC[d] Ref. 88
Dyad	1100-1700	2	0.037	0.531	1.83	0.01	0.23
Pentad	1800-3200	9	0.097	1.109	2.95	0.10	0.29
Octad	3300-4700	24	0.128	1.765	4.66	0.17	0.27
Tetradecad	4800-6200	60	0.167	2.547	…	0.28	0.40
Icosad	6300-7900	134	0.376	3.688	…	0.45	0.66
All	<7900	229	0.303	3.152	…	0.38	0.55

[a] This work (TW) using coupled cluster method with two largest basis sets and including relativistic, DBOC, and high-order correlations contributions (Tables II–IV).

[b] Vibration level calculations by Majumder *et al.*[73] using MRCI-F12(Q)/CVQZ-F12 PES were limited by the Octad range.

[c] Nikitin-Rey-Tyuterev (NRT-2011) PES[72] was obtained by empirical scaling of four parameters to fundamental experimental frequencies, fully converged vibration levels being given in Ref. 127.

[d] Wang-Carrington (WC)[88] have fitted *ab initio* PES of Schwenke[71] to experimental vibrational levels up to the Tetradecad range, the calculations in the Icosad range reported in Ref. 88 being limited by 7550 cm^{-1}. All RMS (obs.-calc.) values are in cm^{-1}.

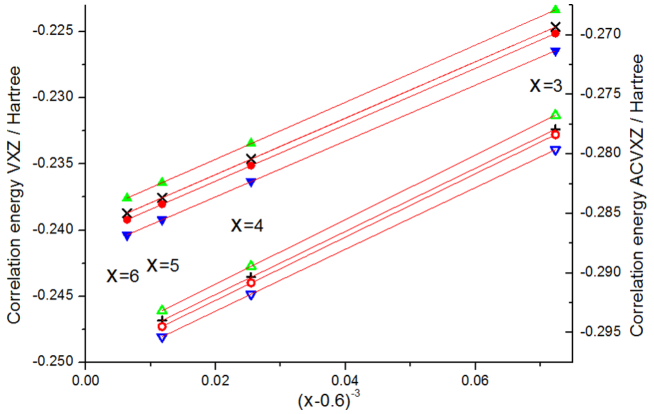

FIG. 7. Basis set dependence of the methane electron correlation energy versus the inverse cubic monomial $(X-0.6)^{-3}$ of the cardinal number. Extrapolations using Eq. (3) are shown by the straight lines whereas the direct $E_c^{(X)}$ *ab initio* calculations using MOLPRO are given by symbols: triangles, crosses, or circles depending on the nuclear geometries. Four upper lines correspond to the VXT basis set series (X = 3, 4, 5, 6), the $E_c^{(X)}$ being given at the left-hand vertical axis. Four lower lines correspond to the ACVXT basis set series (X = 3, 4, 5), the $E_c^{(X)}$ being given at the right-hand vertical axis.

comparison in the reduced wavenumber scale: in Figure 8, we shifted $E_c^{(X)}$ to the zero values at the nuclear equilibrium configuration for each basis set and converted electronic energies in wavenumber units. A detailed analysis shows that this basis set extrapolation works well in a quite uniform way for those geometries in which the radial totally symmetric coordinate SA1_R did not change (in other words if the symmetric stretch "breathing" vibration was not activated). We have made several similar tests playing with different basis set weights but this did not change the results significantly.

This means that if one seeks for *more precise* $E_c^{(X)}$ *extrapolation (accurate within fractions of a wave number in final vibrational levels), the extrapolation law should be geometry dependent*. To best of our knowledge, such an approach has not yet been applied for polyatomic molecules. A part of discrepancies could be removed by introducing in Eq. (3) empirical parameters dependent on SA1_R (with a dominant linear terms at least up to a certain energy). Here we did not follow this way for two reasons. First, this involves arbitrary empirical adjustments that could not be considered as purely *ab initio* results. Another danger is that the geometry dependence of the extrapolated PES becomes more erratic.

C. Non-additivity of fine corrections in different series

Similar extrapolation trends were also obtained for the basis set series ACVDZ, ACVTZ, ACVQZ up to ACV5Z. However, the corresponding straight lines at the lower part of Fig. 7 did not have exactly the same slope as for the VXZ series. In the case of VXZ, we have obtained $b = 0.213$, while we had $b = 0.265$ for ACVXZ in the extrapolation formula (3). This slight difference means that the classical scheme of "additive corrections," which worked quite well for lower basis sets, is no more valid beyond certain accuracy limits. This prevents from using "light" basis set series in order to introduce fine tuning in larger series. The full 9D surface with the largest basis set ACV6Z is currently too expensive. One could approach this goal by two ways: either by extrapolating the series ACVXZ from X = 3, 4, 5 to X = 6 following Eq. (3) or by adding (ACV5Z-V5Z) difference considered as "augmented/core-valence" (AC) correction to directly computed V6Z energies. These two procedures do not give the same results at the end.

On the other hand, we obtained that the corrections (ACV5Z-ACVQZ) and (V5Z-VQZ) behave differently depending on the sub-sets of the geometries in the nuclear configuration space. The illustration of this is given in Fig. 9 that represents the difference in these contributions $\mathrm{diff}_4(S_i) = (\mathrm{ACV5Z}-\mathrm{ACVQZ}) - (\mathrm{V5Z}-\mathrm{VQZ})$ with respect to the samples of grid points.

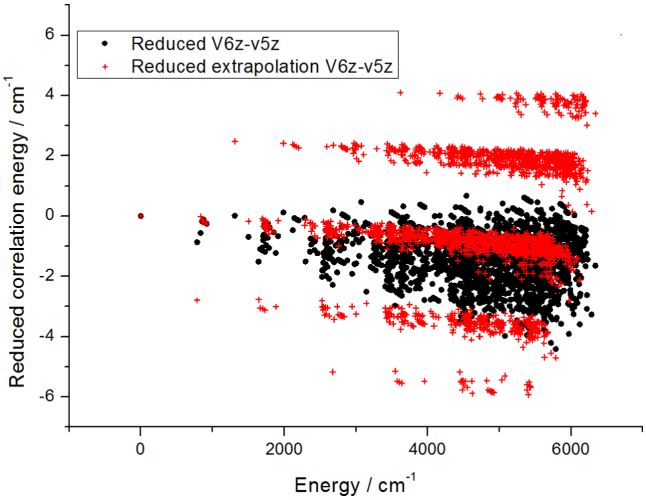

FIG. 8. Geometry dependence of the basis set effect (V6Z-V5Z) in the reduced correlation energies shifted to zero values at the equilibrium nuclear configuration in the vertical scale. The horizontal axis represents total electronic energy at various configurations as computed from the equilibrium point. Black dots correspond to direct *ab initio* calculations using MOLPRO. Red crosses correspond to basis set extrapolations using Eq. (3).

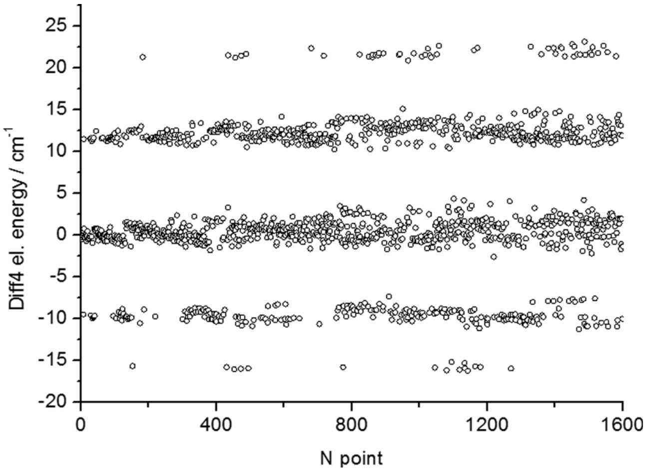

FIG. 9. The non-uniform behavior of the basis set effects in ACVXZ and VXZ series depending on sub-sets of nuclear configurations. The vertical scale gives $\mathrm{diff}_4(S_i) = (\mathrm{ACV5Z}-\mathrm{ACVQZ}) - (\mathrm{V5Z}-\mathrm{VQZ})$ for electron correlation energies. The horizontal axis corresponds to first 1600 points of the nuclear configuration grid with increasing energy.

We have observed that ACVXZ sets gave better results than the V(X + 1)Z sets but extrapolate less smoothly. Our attempts to extrapolate ACVXZ series towards ACV6Z using Eq. (3) resulted in a more erratic PES behavior. The quality of the fit of extrapolated points using the same analytical representation as for X = 4 or X = 5 was deteriorated. This produced a deviation in fundamental vibration levels of about 0.5 cm^{-1}.

VI. CONCLUSIONS

Vibrational predictions using various surfaces (Sec. IV, Tables I–V) suggest the following conclusions. In the case of methane molecule, the high-order dynamic correlations, DBOC, and relativistic corrections give significant contributions (Fig. 6) and are to be included in the 9D PES for achieving band centers accuracy below one wavenumber. Among all basis sets considered in this work, the best results were obtained with ACV5Z. Our final PES computed using CC-ACV5Z and augmented with three above-mentioned contributions is denoted here as "ACV5Z+" PES. We provide this PES in the supplementary material as a C++ code. Variational calculations using this pure *ab initio* surface give very small RMS errors of 0.097 cm^{-1} in the band centers up to the Pentad range (<3200 cm^{-1}), of ~0.17 cm^{-1} in the Tetradecad range (up to 4 excited vibration modes), and of ~0.3 cm^{-1} in the Icosad range (up to 5 excited modes). This representative comparison sample involves all 229 assigned bands up to 7900 cm^{-1}.

No empirically adjusted parameter was involved in the present calculations. To our knowledge, this is the unprecedented accuracy of *ab initio* results for a five-atomic molecule that permitted improving previous *ab initio* calculations for methane bands by more than an order of magnitude (Table V). These *ab initio* predictions are significantly better than vibrational calculations with all published empirically adjusted PESs, even for spectral ranges that were included in their fit. Such a step forward in the computational spectroscopy proves the efficiency of the state-of-art electronic structure methods combined with a thorough sampling of nuclear configuration space, appropriate analytical PES representation, and a full account of the symmetry. With the increasing computer power in future, this approach could be applied for larger polyatomic molecules, in particular for hydrocarbons. This PES will be further used for accurate predictions of new excited ro-vibrational states and transitions in methane at high-temperature conditions important for various astrophysical and combustion applications.[4,35,36,95,37,114,38,19,17,10]

Another conclusion of the study concerns the basis set extrapolations at this level of accuracy. Though VXZ and ACVXZ series qualitatively confirmed the trends of Fig. 7 given by the law (3), our attempts to further improve the accuracy of vibrational predictions using the basis set extrapolations were not fruitful. Various tests described in Secs. V A–V C suggest that basis set extrapolation procedures could be very efficient as a non-expensive way to reduce E_{vib} errors from hundred cm^{-1} to ten cm^{-1} or from ten cm^{-1} to a few wave numbers. However, at present, they are not sufficiently accurate to reduce the errors below 0.1 cm^{-1} that was our purpose. A big issue is that not only extrapolation constants but also the extrapolation formulas should be geometry dependent on targeting such accuracy. In this work, we did not go this way which would require introducing some arbitrary adjustable parameters.

It has been shown[56,46] that an account of non-adiabatic effects[140,141,80,142–144] (and references therein) could further improve the accuracy of calculations, particularly using a semi-empirical scaling of the BO nuclear kinetic energy operator[56,46] by introducing phenomenological parameters that could be different for various inter-nuclear coordinates. As stated in Ref. 46, "these adjustments probably reflect the limited accuracy of the procedure used to determine non-adiabatic corrections." An investigation of these contributions as well of quantum electrodynamic (QED) corrections and of possible compensation of errors in various CBS schemes is beyond the scope of the present work and will be a subject of future studies.

SUPPLEMENTARY MATERIAL

See supplementary material for *ab initio* PES of methane.

ACKNOWLEDGMENTS

The supports of the CNRS (France) and RFBR (Russia) Grant NTsNIL_a 16-53-16022 in the frame of "Laboratoire International Associé SAMIA," of Tomsk State University "Academic D. Mendeleev funding Program," of the "Programme national de planétologie (PNP) du CNRS, of IDRIS/CINES computer centers of France, and of the ROMEO computer center Reims-Champagne-Ardenne are acknowledged. A.V.N. thanks Champagne-Ardenne Region and the University of Reims for support.

[1] M. Quack and J. Troe, Ber. Bunsenges. Phys. Chem. **81**, 329 (1977).
[2] T. Nishimura and F. A. Gianturco, Phys. Rev. A **65**, 062703 (2002).
[3] H. Schwarz, Angew. Chem., Int. Ed. **50**, 10096–10115 (2011).
[4] E. Jourdanneau, T. Gabard, F. Chaussard, R. Saint-Loup, H. Berger, E. Bertseva, and F. Grisch, J. Mol. Spectrosc. **246**, 167 (2007).
[5] C. Sagan, R. W. Thompson, R. Carlson, D. Gurnett, and C. Hord, Nature **365**, 715 (1993).
[6] G. C. Rhoderick and W. D. Dorko, Environ. Sci. Technol. **38**, 2685 (2004).
[7] D. J. Nesbitt and R. W. Field, J. Phys. Chem. **100**, 12735 (1996).
[8] M. Khalil, Annu. Rev. Energy Environ. **24**, 645–661 (1999).
[9] O. Boucher, P. Friedlingstein, B. Collins, and K. P. Shine, Environ. Res. Lett. **4**, 044007 (2009).
[10] G. Tinetti, T. Encrenaz, and A. Coustenis, Astron. Astrophys. Rev. **21**, 63 (2013).
[11] C. De Bergh *et al.*, Planet. Space Sci. **61**, 85–98 (2012).
[12] M. Hirtzig *et al.*, Icarus **226**, 470–486 (2013).
[13] F. Allard, P. H. Hauschildt, D. R. Alexander, and S. Starrfield, Annu. Rev. Astron. Astrophys. **35**, 137 (1997).
[14] B. R. Oppenheimer, S. R. Kulkarni, K. Matthews, and T. Nakajima, Science **270**, 1478 (1995).
[15] M. R. Swain, G. Vasisht, and G. Tinetti, Nature **452**, 329–333 (2008).
[16] R. Hu and S. Seager, Astrophys. J. **784**, 1 (2014).
[17] B. Macintosh, J. R. Graham, and T. Barman, Science **350**, 64–67 (2015).
[18] S. L. Mielke and D. G. Truhlar, J. Chem. Phys. **142**, 044105 (2015).
[19] P. F. Bernath, Philos. Trans. R. Soc., A **372**, 20130087 (2014).
[20] I. P. Waldmann, G. Tinetti, P. Drossart, M. R. Swain, P. Deroo, and C. A. Griffith, Astrophys. J. **744**, 35 (2012).

[21] A. V. Nikitin, V. Boudon, Ch. Wenger, S. Albert, L. R. Brown, S. Bauerecker, and M. Quack, Phys. Chem. Chem. Phys. **15**, 10071–10093 (2013).

[22] Vl. G. Tyuterev, R. V. Kochanov, S. A. Tashkun, F. Holka, and P. G. Szalay, J. Chem. Phys. **139**, 134307 (2013).

[23] M. Rey, A. V. Nikitin, and Vl. G. Tyuterev, Phys. Chem. Chem. Phys. **15**, 10049–10061 (2013).

[24] M. Rey, A. V. Nikitin *et al.*, Phys. Chem.Chem. Phys. **18**, 176–189 (2016).

[25] S. Albert, S. Bauerecker, V. Boudon, L. R. Brown, J.-P. Champion, M. Loete, A. V. Nikitin, and M. Quack, Chem. Phys. **358**, 131–146 (2009).

[26] L. Daumont *et al.*, J. Quant. Spectrosc. Radiat. Transfer **116**, 101–109 (2013).

[27] A. V. Nikitin, M. Rey, S. A. Tashkun, S. Kassi, D. Mondelain, A. Campargue *et al.*, J. Quant. Spectrosc. Radiat. Transfer **168**, 207–216 (2016).

[28] A. V. Nikitin, J. P. Champion, Vl. G. Tyuterev, L. R. Brown, G. Mellau, and M. Lock, J. Mol. Struct. **517-518**, 1–24 (2000).

[29] H.-M. Niederer, S. Albert, S. Bauerecker, V. Boudon, J.-P. Champion, and M. Quack, Chimia **62**, 273–276 (2008).

[30] A. V. Nikitin, J.-P. Champion, and L. R. Brown, J. Mol. Spectrosc. **240**, 14–25 (2006).

[31] L. R. Brown *et al.*, J. Quant. Spectrosc. Radiat. Transfer **174**, 88–100 (2016).

[32] E. Starikova, A. V. Nikitin, M. Rey, S. A. Tashkun, D. Mondelain, S. Kassi, A. Campargue, and Vl. G. Tyuterev, J. Quant. Spectrosc. Radiat. Transfer **177**, 170 (2015).

[33] V. I. Perevalov, Vl. G. Tyuterev, and B. I. Zhilinskii, Chem. Phys. Lett. **104**, 455–461 (1984).

[34] V. I. Perevalov, Vl. G. Tyuterev, and B. I. Zhilinskii, J. Mol. Spectrosc. **111**, 1–19 (1985).

[35] R. Nassar and P. Bernath, J. Quant. Spectrosc. Radiat. Transfer **82**, 279–282 (2003).

[36] J. Thievin, R. Georges, S. Carles, B. Abdessamad, B. Rowe, and J. P. Champion, J. Quant. Spectrosc. Radiat. Transfer **109**, 2027 (2008).

[37] R. J. Hargreaves, C. A. Beale, L. Michaux, M. Irfan, and P. F. Bernath, Astrophys. J. **757**, 46 (2012).

[38] R. J. Hargreaves, P. F. Bernath, and D. R. T. Appadoo, J. Mol. Spectrosc. **315**, 102 (2015).

[39] B. Amyay, M. Louviot, O. Pirali, R. Georges, J. Vander Auwera, and V. Boudon, J. Chem. Phys. **144**, 024312 (2016).

[40] D. N. Kozlov, D. A. Sadovskii, and P. P. Radi, J. Mol. Spectrosc. **291**, 23–32 (2013).

[41] O. N. Ulenikov, E. S. Bekhtereva, S. Albert, S. Bauerecker, H. M. Niederer, and M. Quack, J. Chem. Phys. **141**, 234302 (2014).

[42] L. R. Brown *et al.*, J. Quant. Spectrosc. Radiat. Transfer **130**, 201–219 (2013).

[43] H. Partridge and D. W. Schwenke, J. Chem. Phys. **106**, 4618–4639 (1997).

[44] O. L. Polyansky, N. F. Zobov, S. Viti, J. Tennyson, P. F. Bernath, and L. Wallace, Science **277**, 346–348 (1997).

[45] J. Tennyson, P. Barletta, M. A. Kostin, O. L. Polyansky, and N. F. Zobov, Spectrochim. Acta, Part A **58**, 663–672 (2002).

[46] O. Polyansky, R. Ovsyannikov, A. Kyuberis, L. Lodi, J. Tennyson, and N. Zobov, J. Phys. Chem. A **117**, 9633–9643 (2013).

[47] X. Huang, D. W. Schwenke, S. A. Tashkun *et al.*, J. Chem. Phys. **136**, 124311 (2012).

[48] X. Huang, R. S. Freedman, S. A. Tashkun, D. W. Schwenke, and T. J. Lee, J. Quant. Spectrosc. Radiat. Transfer **139**, 134–146 (2013).

[49] S. N. Yurchenko, R. J. Barber, A. Yachmenev, W. Thiel, P. Jensen, and J. Tennyson, J. Phys. Chem. A **113**, 11845–11855 (2009).

[50] T. Cours, P. Rosmus, and Vl. G. Tyuterev, J. Chem. Phys. **117**, 5192 (2002).

[51] A. A. Azzam, L. Lodi, S. N. Yurchenko, and J. Tennyson, J. Quant. Spectrosc. Radiat. Transfer **161**, 41–49 (2015).

[52] D. W. Schwenke, T. J. Lee, and X. C. Huang, J. Chem. Phys. **140**, 114311 (2014).

[53] A. Campargue, A. Barbe, M. R. De Backer-Barilly, Vl. G. Tyuterev, and S. Kassi, Phys. Chem. Chem. Phys. **10**, 2925–2946 (2008).

[54] Vl. G. Tyuterev, R. V. Kochanov, A. Campargue, S. Kassi, D. Mondelain, and A. Barbe, Phys. Rev. Lett. **113**, 143002 (2014).

[55] R. Dawes, P. Lolur, J. Ma, and H. Guo, J. Chem. Phys. **135**, 081102 (2011).

[56] X. Huang, D. W. Schwenke, and T. J. Lee, J. Chem. Phys. **134**, 044320 (2011).

[57] S. N. Yurchenko, M. Carvajal, W. Thiel, and P. Jensen, J. Mol. Spectrosc. **239**, 71–87 (2006).

[58] C. Sousa-Silva, S. N. Yurchenko, and J. Tennison, J. Mol. Spectrosc. **288**, 28–36 (2013).

[59] A. V. Nikitin, M. Rey, and Vl. G. Tyuterev, J. Mol. Spectrosc. **305**, 40–47 (2014).

[60] A. Owens, S. N. Yurchenko, A. Yachmenev, J. Tennyson, and W. Thiel, J. Chem. Phys. **142**, 244306 (2015).

[61] A. Owens, S. N. Yurchenko, A. Yachmenev, and W. Thiel, J. Chem. Phys. **143**, 244317 (2015).

[62] T. Delahaye, A. Nikitin, M. Rey, P. Szalay, and Vl. G. Tyuterev, J. Chem. Phys. **141**, 104301 (2014).

[63] T. Delahaye, A. V. Nikitin, M. Rey, P. G. Szalay, and Vl. G. Tyuterev, Chem. Phys. Lett. **639**, 275–282 (2015).

[64] J. Li, S. Carter, J. M. Bowman, R. Dawes, D. Xie, and H. Guo, J. Phys. Chem. Lett. **5**, 2364–2369 (2014).

[65] L. M. Raff, R. Viswanathan, and D. L. Thompson, J. Chem. Phys. **80**, 6141 (1984).

[66] S. Brodersen and J. E. Lolck, J. Mol. Spectrosc. **126**, 405 (1987).

[67] H. Furue, J. F. LeBlanc, P. D. Pacey, and J. M. Whalen, Chem. Phys. **154**, 425 (1991).

[68] M. J. T. Jordan and R. G. Gilbert, J. Chem. Phys. **102**, 5669 (1995).

[69] T. J. Lee, J. M. L. Martin, and P. R. Taylor, J. Chem. Phys. **102**, 254 (1995).

[70] R. Marquardt and M. Quack, J. Phys. Chem. **108**, 3166–3181 (2004).

[71] D. W. Schwenke and H. Partridge, Spectrochim. Acta, Part A **57**, 887–895 (2001).

[72] A. V. Nikitin, M. Rey, and Vl. G. Tyuterev, Chem. Phys. Lett. **501**, 179–186 (2011).

[73] M. Majumder, S. E. Hegger, R. Dawes, S. Manzhos, X.-G. Wang, T. Carrington, Jr., J. Lid, and H. Guo, Mol. Phys. **113**, 1823–1833 (2015).

[74] P. Cassam-Chenai and J. Lievin, J. Chem. Phys. **136**, 174309 (2012).

[75] S. N. Yurchenko, J. Tennyson, R. J. Barber, and W. Thiel, J. Mol. Spectrosc. **291**, 69–76 (2013).

[76] A. V. Nikitin, M. Rey, and Vl. G. Tyuterev, Chem. Phys. Lett. **565**, 5–11 (2013).

[77] R. Marquardt and M. Quack, J. Chem. Phys. **109**, 10628 (1998).

[78] M. Lewerenz and M. Quack, J. Chem. Phys. **88**, 5408–5432 (1988).

[79] M. Lewerenz, R. Marquardt, and M. Quack, J. Chem. Soc., Faraday.Trans. **84**, 1580–1583 (1988).

[80] D. W. Schwenke, Spectrochim. Acta, Part A **58**, 849–861 (2002).

[81] X. Wang and L. Edwin Sibert III, Spectrochim. Acta, Part A **58**, 863–872 (2002).

[82] J. M. Bowman, T. Carrington, and H.-D. Meyer, Mol. Phys. **106**, 2145 (2008).

[83] E. Matyus, J. Simunek, and A. Csaszar, J. Chem. Phys. **131**, 074106 (2009).

[84] X.-G. Wang and T. Carrington, Jr., J. Chem. Phys. **138**, 104106 (2013).

[85] C. Oyanagi, K. Yagi, T. Taketsugu, and K. Hirao, J. Chem. Phys. **124**, 064311 (2006).

[86] J. Troe, Mol. Phys. **112**, 2374–2383 (2014).

[87] X.-G. Wang and E. L. Sibert III, J. Chem. Phys. **111**, 4510–4522 (1999).

[88] X.-G. Wang and T. Carrington, Jr., J. Chem. Phys. **141**, 154106 (2014).

[89] S. N. Yurchenko and J. Tennyson, Mon. Not. R. Astron. Soc. **440**, 1649–1661 (2014).

[90] M. Rey, A. V. Nikitin, and Vl. G. Tyuterev, J. Phys. Chem. A **119**, 4763–4779 (2015).

[91] M. Rey, A. V. Nikitin, and Vl. G. Tyuterev, J. Mol. Spectrosc. **291**, 85–97 (2013).

[92] M. Rey, A. V. Nikitin, and Vl. G. Tyuterev, J. Chem. Phys. **141**, 044316 (2014).

[93] M. Rey, A. V. Nikitin, and Vl. G. Tyuterev, Astrophys. J. **789**, 2 (2014).

[94] M. Rey, A. V. Nikitin, Y. Babikov, and Vl. G. Tyuterev, J. Mol. Spectrosc. **327**, 138–158 (2016).

[95] R. Warmbier, R. Scheider, A. R. Sharma *et al.*, Astron. Astrophys. **495**, 665 (2009).

[96] Ch. Wenger, J. P. Champion, and V. Boudon, J. Quant. Spectrosc. Radiat. Transfer **109**, 2697–2706 (2008).

[97] A. V. Nikitin *et al.*, J. Quant. Spectrosc. Radiat. Transfer **154**, 63–71 (2015).

[98] G. D. Purvis and R. J. Bartlett, J. Chem. Phys. **76**, 1910 (1982).

[99] T. H. Dunning, J. Chem. Phys. **90**, 1007 (1989).

[100] T. B. Adler, G. Knizia, and H.-J. Werner, J. Chem. Phys. **127**, 221106 (2007).

[101] G. Knizia, T. Adler, and H. Werner, J. Chem. Phys. **130**, 054104 (2009).

[102] J. G. Hill, K. A. Peterson, G. Knizia, and H.-J. Werner, J. Chem. Phys. **131**, 194105 (2015).

[103] H.-J. Werner, P. J. Knowles, G. Knizia, F. R. Manby *et al.*, Wiley Interdiscip. Rev.: Comput. Mol. Sci. **2**, 242–253 (2012).

[104] A. V. Nikitin, F. Holka, Vl. G. Tyuterev, and J. Fremont, J. Chem. Phys. **131**, 244312 (2009).

[105] M. Reiher and A. Wolf, J. Chem. Phys. **121**, 10945 (2004).

[106] R. D. Cowan and D. C. Griffin, J. Opt. Soc. Am. **66**, 1010–1014 (1976).

[107] W. Kutzelnigg, Mol. Phys. **90**, 900–916 (1997).

[108] J. F. Stanton, J. Gauss, M. E. Harding, P. G. Szalay *et al.*, CFour program, http://www.cfour.de; J. Gauss, A. Tajti, M. Kallay, J. F. Stanton, and P. G. Szalay, J. Chem. Phys. **125**, 144111 (2006).

[109] D. A. Matthews and J. F. J. F. Stanton, J. Chem. Phys. **142**, 064108 (2015); Y. J. Bomble, J. F. Stanton, M. Kallay, and J. Gauss, J. Chem. Phys. **123**, 054101 (2005).

[110] M. Kállay and P. R. Surján, J. Chem. Phys. **115**, 2945 (2001); Mrcc, a quantum chemical program suite written by M. Kallay, Z. Rolik, J. Csontos, I. Ladjanszki, L. Szegedy, B. Ladoczki, G. Samu, K. Petrov, M. Farkas, P. Nagy, D. Mester, and B. Hegely. See also Z. Rolik, L. Szegedy, I. Ladjanszki, B. Ladoczki, and M. Kallay, J. Chem. Phys. **139**, 094105 (2013), as well as: www.mrcc.hu.

[111] J. F. Stanton, Mol. Phys. **97**, 841–845 (1999).

[112] A. V. Nikitin, M. Rey, and Vl. G. Tyuterev, J. Chem. Phys. **142**, 094118 (2015).

[113] A. V. Nikitin, J. P. Champion, and Vl. G. Tyuterev, J. Mol. Spectrosc. **182**, 72–84 (1997).

[114] J.-P. Champion, M. Loete, and G. Pierre, *Spectroscopy of the Earth's Atmosphere and Interstellar Medium* (Academic Press, San Diego, 1992).

[115] B. I. Zhilinskii, V. I. Perevalov, and Vl. G. Tyuterev, *Method of Irreducible Tensorial Operators in the Theory of Molecular Spectra* (Nauka, Novosibirsk, 1987).

[116] V. Boudon, J. P. Champion, T. Gabard, M. Loete, F. Michelot, G. Pierre *et al.*, J. Mol. Spectrosc. **228**, 620–634 (2004).

[117] M. Rey, A. V. Nikitin, and Vl. G. Tyuterev, J. Chem. Phys. **136**, 244106 (2012).

[118] D. A. Sadovskii and B. I. Zhilinskii, Mol. Phys. **65**, 109–128 (1988).

[119] D. A. Sadovskii, B. I. Zhilinskii, J. P. Champion, and G. Pierre, J. Chem. Phys. **92**, 1523–1537 (1990).

[120] Vl. G. Tyuterev, S. A. Tashkun, M. Rey, R. V. Kochanov, A. V. Nikitin, and T. Delahaye, J. Phys. Chem. **117**, 13779–13805 (2013).

[121] X. G. Wang and T. Carrington, Jr., J. Chem. Phys. **121**, 2937–2954 (2004).

[122] S. Carter, J. Chem. Phys. **110**, 8417–8423 (1999).

[123] S. Carter, A. R. Sharma, and J. M. Bowman, J. Chem. Phys. **137**, 154301 (2012).

[124] J. K. G. Watson, Mol. Phys. **15**, 479 (1968).

[125] H.-G. Yu, J. Chem. Phys. **117**, 2030–2037 (2002).

[126] H.-G. Yu, J. Chem. Phys. **121**, 6334–6340 (2004).

[127] M. Rey, A. V. Nikitin, and Vl. G. Tyuterev, J. Quant. Spectrosc. Radiat. Transfer **164**, 207–220 (2015).

[128] A. V. Nikitin, M. Rey, J.-P. Champion, and Vl. G. Tyuterev, J. Quant. Spectrosc. Radiat. Transfer **113**, 1034–1042 (2012).

[129] M. Rey, A. V. Nikitin, and Vl. G. Tyuterev, Mol. Phys. **108**, 2121–2135 (2010).

[130] Vl. G. Tyuterev and V. I. Perevalov, Chem. Phys. Lett. **74**, 494–502 (1980).

[131] W. G. Harter and C. W. Patterson, J. Chem. Phys. **80**, 4241–4261 (1984).

[132] P. Cassam-Chenai, G. Rousseau, A. Ilmane, Y. Bouret, and M. Rey, J. Chem. Phys. **143**, 034107 (2015).

[133] A. V. Nikitin, X. Thomas, L. Regalia, L. Daumont, M. Rey, S. A. Tashkun, Vl. G. Tyuterev, and L. R. Brownc, J. Quant. Spectrosc. Radiat. Transfer **138**, 116–123 (2014).

[134] A. V. Nikitin, X. Thomas, L. Regalia, L. Daumont, P. Von der Heyden, and Vl. G. Tyuterev, J. Quant. Spectrosc. Radiat. Transfer **112**, 28–40 (2011).

[135] A. V. Nikitin *et al.*, J. Quant. Spectrosc. Radiat. Transfer **111**, 2211–2224 (2010).

[136] J. M. L. Martin, Chem. Phys. Lett. **259**, 669–678 (1996).

[137] D. G. Truhlar, Chem. Phys. Lett. **294**, 45 (1998).

[138] A. Halkier, T. Helgaker, P. Jørgensen, W. Klopper, and J. Olsen, Chem. Phys. Lett. **302**, 437–446 (1999).

[139] D. W. Schwenke, J. Chem. Phys. **122**, 014107 (2005).

[140] D. W. Schwenke, J. Phys. Chem. A **105**, 2352–2360 (2001).

[141] W. Kutzelnigg, Mol. Phys. **105**, 2627–2647 (2007).

[142] F. Holka, P. Szalay, J. Fremont, M. Rey, K. Peterson, and Vl. G. Tyuterev, J. Chem. Phys. **134**, 094306 (2011).

[143] L. G. Diniz, N. Kirnosov, A. Alijah, J. R. Mohallem, and L. Adamowicz, J. Mol. Spectrosc. **322**, 22–28 (2016).

[144] A. Alijah, J. Fremont, and Vl. G. Tyuterev, Phys. Rev. A **92**, 012704 (2015).